ELSEVIER

Remote Sensing of Environment

www.elsevier.com/locate/rse

Northern Forest Ecosystem Dynamics Using Coupled Models and Remote Sensing

K. J. Ranson, G. Sun,† R. G. Knox,* E. R. Levine,* J. F. Weishampel,‡ and S. T. Fifer§*

Forest ecosystem dynamics modeling, remote sensing data analysis, and a geographical information system (GIS) were used together to determine the possible growth and development of a northern forest in Maine, USA. Field measurements and airborne synthetic aperture radar (SAR) data were used to produce maps of forest cover type and above ground biomass. These forest attribute maps derived with remote sensing data, along with a conventional soils map, were used to identify the initial conditions for forest ecosystem model simulations. Using this information along with ecosystem model results enabled the development of predictive maps of forest development. The results obtained were consistent with observed forest conditions and expected successional trajectories. The study demonstrated that ecosystem models might be used in a spatial context when parametrized and used with georeferenced data sets.

INTRODUCTION

The circumpolar boreal forest is one of the Earth's major vegetative ecosystems, accounting for nearly 20% of the terrestrial plant carbon and covering one-sixth of the Earth's land surface (Bolin, 1986). The northern and southern margins are especially sensitive to climate change as evidenced by the northward migration of boreal species since the end of the Wisconsin Ice Age (Pastor and Mladenoff, 1992). There is now evidence that growing season duration and vegetation growth are increasing in the high latitudes (Myneni et al., 1997). Increasing harvesting pressures coupled with the ever-present impacts of forest fires and insect outbreaks are changing the face of forests everywhere. The nature and extent of the impacts of these changes, as well as the feedback on global climate, are not well understood, but may be addressed through modeling the interactions of the vegetation, soil, and energy components of ecosystems (Pastor and Post, 1988; Bonan et al., 1995; Trumbore et al., 1996). The use of combined ecosystem and remote sensing models presents an especially efficient and tractable method to study regional and global environmental changes.

The Forest Ecosystem Dynamics (FED) Project at Goddard Space Flight Center (GSFC) involves the development and integration of models to understand soil, vegetation, and radiation dynamics in northern forest ecosystems. Through the use of simulation models, remote sensing, field investigation, and GIS, the vegetation, soil, and energy components within northern forests are being investigated, and their responses to global change and other disturbances are being explored and quantified (e.g., Levine et al., 1993; Levine and Knox, 1997). The development and implementation of a framework for combining models that simulate various ecosystem processes (Workbench for Interactive Simulation of Ecosystems, WISE) was described by Knox et al. (1997). Work has continued that uses ecosystem model simulations along with remote sensing models to explore remote sensing algorithm development (Ranson and Sun, 1997a; Kimes et al., 1997).

In this work, data collection and model development have focused on northern forests of North America including Maine, USA and Saskatchewan, Canada (e.g.,

* NASA Goddard Space Flight Center, Greenbelt, Maryland
† University of Maryland, Department of Geography, College Park, Maryland
‡ University of Central Florida, Department of Biology, Orlando, Florida
§ Raytheon ITSS, Lanham, Maryland

Address correspondence to K. J. Ranson, NASA Goddard Space Flight Ctr., Code 923, Greenbelt, MD 20771. E-mail: jon@taiga.gsfc.nasa.gov
Received 14 September 1999; revised 21 July 2000.

REMOTE SENS. ENVIRON. 75:291–302 (2001)

655 Avenue of the Americas, New York, NY 10010

0034-4257/00/$–see front matter
PII S0034-4257(00)00174-7

Goward et al., 1994; Ranson and Sun, 1997b). Intensive field measurements coinciding with aircraft and satellite overflights, as well as ancillary data, were obtained and incorporated into a GIS. The GIS is used to provide driving variables for the models, initialize model runs, validate model predictions, and identify areas requiring more intensive study.

In the present study we demonstrate a technique for connecting models of forest dynamics and soil processes along with remotely sensed forest attributes in a spatially explicit manner. Kasischke and Christensen (1990) outlined, in general terms, steps to connect forest ecosystem models with radar backscatter models. They suggested the use of forest growth models to help develop and validate backscatter models that predict the radar signature based on tree stand characteristics. The objective of their proposed technique was to provide inputs to forest models. He and Mladenoff (1999) have developed a spatially explicit landscape model to study fire history in Wisconsin that uses forest cover derived from classified Landsat data as input. We describe the use of remote sensing derived maps of forest type and biomass used with ancillary data to initialize and test a forest dynamics model.

This article is organized into four sections including the introduction. The Background section provides brief descriptions of the modeling components, the coupled model environment, and the remote sensing and field data. The Methods section describes the implementation of the forest succession model, the analysis of remote sensing data, and the prediction of forest dynamics. The maps derived from remote sensing and predictive maps of forest dynamics are discussed in the Results section.

BACKGROUND

Forest Dynamics Modeling

Mathematical models that simulate forest dynamics have gained widespread acceptance and use over the past two decades. The most successful models (in terms of general applicability to diverse forest types) are individual tree-based models called gap models (Shugart et al., 1992; Botkin, 1993; Deutschman et al., 1997). The strength of these models lies in their versatility to predict qualitative successional patterns related to species composition and forest structure.

The gap model, ZELIG (Urban, 1990), is an individual tree simulator that simulates the annual establishment, annual diameter growth, and mortality of each tree on an array of model plots. Model states are recorded in a tally of all trees on a plot, with each tree labeled by species, size (diameter), height to base of live crowns, and vigor (based on recent growth history). The competitive environment of the plot is defined by the height, leaf area, and woody biomass of each individual tree determined by allometric relationships with diameter. The plot is considered homogeneous horizontally, but vertical heterogeneity (canopy height and vertical distribution of leaf area) is simulated in some detail. Establishment and annual diameter growth is first computed under optimal (nonlimiting) conditions, and then reduced based on the constraints of available light, soil moisture, soil fertility, and temperature. Annual climate effects are summed across simulated months. Seedling establishment, mortality, and regeneration are computed stochastically, while growth is largely deterministic. Simulations can start or stop at any point within the life cycle of a forest. However for simulations beginning from other than bare ground, details on existing forest status (e.g., species composition diameter breast height, size class distribution) are necessary for model initialization.

Soil Process Modeling

The goal of simulating the soil system beneath the forest is to understand the controls and feedbacks that operate within the soil as well as between the soil and the rest of the forest environment. This includes physical, biological, chemical, and mineralogical characteristics and mechanisms that vary at short-, medium-, and long-term temporal scales within soils. The FroST (Frozen Soil Temperatures) model (Levine and Knox, 1997), which includes the physical processes occurring within the soil, was used within the FED modeling framework. FroST is a simulation model of soil properties which produces estimates of water content, matric potential, temperature, and ice content within each soil horizon. FroST was developed from the Residue model of Bidlake et al. (1992) which couples surface residue to the soil–atmosphere system, and uses network analysis to describe heat and moisture transfer, and phase changes in water. Short-wave and long-wave radiative transfer, changes in energy status, rainfall interception, infiltration, redistribution, evaporation, and drainage are all accounted for. Climate input requirements include global short-wave radiation, air temperatures, average wind speed, and precipitation. General site, canopy, and soil characteristics for individual horizons are also needed. Enhancements to the Residue model to produce FroST included algorithms for calculating surface runoff, transpiration, Penman demand, and a simple snow model. In FroST, surface residue from the Residue model is configured to simulate above ground characteristics of forested sites. Snow properties are simulated by changing the characteristics of the surface soil node from soil characteristics to snow characteristics. Precipitation increases the node's thickness (i.e., snow cover), and a simple melt factor is used to melt the snow. Once the snow has melted, node characteristics are reset to that of soil (Levine and Knox, 1997). The ability of the model to handle moisture and temperature profiles also makes it suitable for use in permafrost simulations as we move our studies to true boreal environments.

Modeling Environment

To interactively integrate and use the forest succession and soil process models, both models were incorporated into the Forest Ecosystem Dynamics' WISE (Workbench for Interactive Simulation of Ecosystems) modeling environment. WISE supports interactive configuration, manages the transfer of variables among models, and dynamically displays results (Levine et al., 1993; Knox et al., 1997). The modeling environment allows two or more process models to be coupled using a generic query–response system where parameter values from detailed models in one discipline can be provided to drive models of other disciplines. Models are encapsulated and then run synchronously from a common external clock. Databaselike features added while encapsulating each model allow models to query one another while running. Each encapsulated model also has X-windows panels defining a model-specific graphical "subinterface" and a version of a configuration tool to check parameter values entered interactively against rule sets defining allowable combinations of values. (Example WISE panels may be viewed over the Internet via http://fedwww.gsfc.nasa.gov). Currently, several models are encapsulated including ZELIG and FroST. With this modeling tool, scaling parameters from detailed models can be derived to improve values used in simpler models for the same parameter.

Remote Sensing

During the NASA Multisensor Aircraft campaign in 1989–1990 SIR-C/XSAR Mission (1994), several AIRSAR or SIR-C/XSAR images were acquired. These data, along with field measurements, were used to produce maps of forest cover type (Ranson and Sun, 1994a) and aboveground biomass (Ranson and Sun, 1994b; 1997). Temporal (winter and summer) multifrequency polarimetric AIRSAR data were used to produce a map of the study area with general forest categories such as softwood, hardwood, regeneration, and other nonforest categories with better than 80% accuracy (Ranson and Sun, 1994a). The forest areas of this classification map were compiled into three major forest categories, that is, conifer, deciduous, and mixture for the purpose of this study. Similar maps could be produced using other remote sensing data, such as the Landsat TM data.

Radar provides a unique tool for accessing northern forest biomass since it is unaffected by cloud or low solar zenith angle and penetrates farther into forest canopies than optical wavelengths. Studies (e.g., Dobson et al., 1992; Le Toan et al., 1992; Rignot et al., 1994) have shown good correlations of radar backscatter and biomass for different forest stands. Generally, it is found that longer wavelength cross-polarization radar backscatter was the most sensitive to woody biomass. Ranson and Sun (1994b) have shown that the combinations of longer and shorter wavelength SAR data may reduce the effect of incidence angle. A biomass map developed from SAR data was used as current base map in this study (Ranson and Sun, 1997).

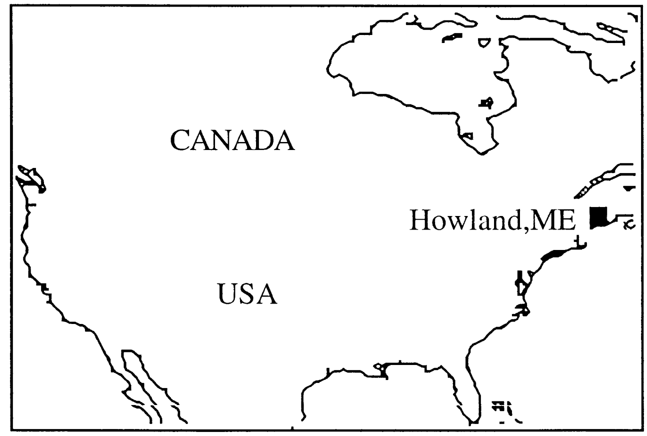

Figure 1. Location of study site in the northeastern USA.

Study Area

The area under study is located at the International Paper Northern Experimental Forest (NEF) near Howland, Maine, USA (Fig. 1). The site is located at approximately 45°15′N latitude and 68°45′W longitude. The area comprises approximately 7000 ha containing several intensive experimental sites, where detailed ecological and mensuration measurements have been obtained. It contains an assortment of small plantations, multigeneration clearings, and large natural southern boreal-northern hardwood transition forest stands consisting of hemlock–spruce–fir, aspen–birch, and hemlock–hardwood mixtures. Topographically, the region varies from flat to gently rolling, with a maximum elevation change of less than 135 m within a 10 km by 10 km study area. Due to the region's glacial history, soil drainage classes within a small area may vary widely, from excessively drained to poorly drained.

There exists a wide variety of imagery, map data, and point data at the NEF and surrounding areas within a Geographic Information System (GIS) for research purposes. These data include field, tower, aircraft and satellite based measurements and are described and distributed from the FED project's GIS database also available through the Internet at http://fedwww.gsfc.nasa.gov.

METHODS

In this article we demonstrate that parameter maps developed from remotely sensed data can be used to initial-

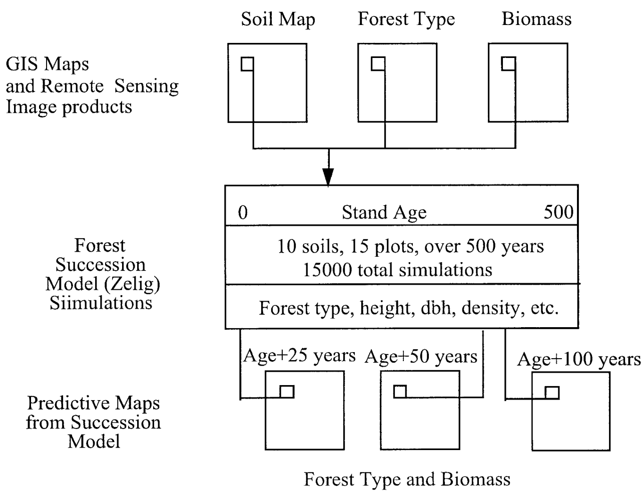

Figure 2. Diagram of procedures for using maps of forest attributes developed from remote sensing and soil survey maps to initialize a forest succession model and develop maps of future forest type and biomass.

ize and test a forest succession model. Figure 2 outlines the methods used for the study reported here. First, remote sensing data were analyzed for forest type and biomass levels and maps were developed. Second, a forest model (ZELIG) was coupled to the soil physics model (FroST) and run for a range of soil conditions found at the site over a 500-year period (see Weishampel et al., 1999). Individual pixels from the forest type and biomass maps along with a soil type map were compared with the results of the forest model to determine the age of the forest represented by the pixel. These age and forest conditions were used for model initialization, and simulation results for 100 years in the future (using current climate) were recorded. The individual steps of the method are described in the following sections.

Remote Sensing Analysis

AIRSAR Data. We used data from the JPL AIRborne Synthetic Aperture Radar (AIRSAR) instrument because it was readily available for our test site and there was good supporting ground truth. The data was acquired to support a SIR-C/XSAR study (see Ranson and Sun, 1997). AIRSAR was flown over the NEF onboard a DC-8 aircraft on 15 April 1994 and 7 October 1994 [see Way and Smith (1991) for a description of aircraft and sensor]. The AIRSAR acquired backscatter data at C-band (wavelength=5.6 cm, frequency=5.3 GHz), L-band (23.9 cm, 1.25 GHz), and P-band (67.0 cm, 0.44 GHz) in four polarizations (HH, VV, HV, VH). Both flights acquired data at about 10:00 a.m. local time (EDT) under warm and dry weather conditions. The AIRSAR data were processed by JPL's Radar Data Center and provided in multilook compressed Stokes matrix format. Upon receipt of the data from JPL, we extracted single channel images and converted slant range to ground range. The resulting images had a nominal resolution of 8.3 m and covered an area of about 8.5 km in the along track direction and 12 km in the across track direction. We used data that covered 9 km by 6.4 km to avoid data at steep radar incidence angles (i.e., $<30°$).

Image Registration. Image registration was required to use multidate AIRSAR images. Since our research area has low topographic relief (maximum change in elevation of 145 m over 10 km), and the flight directions and incidence angle ranges of the pair of images were similar, the registration was easily accomplished. A linear interpolation with about 10 control points yielded results superior to a cubic polynomial interpolation with 20 control points. The conditions during the AIRSAR flights apparently were quite stable and the distortion was linear. The April AIRSAR image was registered to the October AIRSAR.

Forest Type Classification. Ranson and Sun (1994a) produced a forest type map of the Howland area using AIRSAR images. They found that combining summer and winter images produced better results than using data from a single date. They used principal components analysis to reduce the number of channels used with a maximum likelihood classifier. In this study, all nonredundant channels from both dates were used with a supervised minimum distance classifier.

A parallelepiped classifier (Moik, 1980), which approximates the hyperellipsoid decision boundaries of Bayesian classifier by parallelepipeds, was used similar to that reported by Ranson and Sun (1997). Nine land cover classes were selected from a generalized cover type map provided by International Paper: water, bog, wetland, grassland, clearing, regeneration, mixed forest, hardwood forest, and softwood forest. The latter five classes represent the state of the forest stands in the area from harvest through regrowth (regeneration) to mature "monospecies" or mixed stands.

The classifier was trained for the nine classes by locating areas identified from forest cover maps, aerial photos and field observations on the SAR imagery. As described above, the AIRSAR image data was acquired with 12 channels (C-, L- and P-band with HH, HV, VV, VH polarizations). The set of channels for this analysis used only one cross polarization channel (VH) for each frequency. The registered forest type map was placed in the GIS for further use.

Above Ground Biomass Mapping. Forest stands, measured during 1992 and 1994, were located on AIRSAR images, and 3×3 block of pixels were extracted from which the average backscatter was calculated. The field biomass data was acquired from stands of predominantly spruce and hemlock and mixtures of hemlock and hardwood species.

An earlier analysis of AIRSAR data over the Maine study area estimated above ground standing biomass from a combination of radar channels (Ranson and Sun, 1994b). A combination of P-band HV and C-band HV (i.e., PHV–CHV in dB) was found to have the best sensitivity to total above ground biomass. Briefly, the procedure involves developing a linear regression equation with biomass and SAR backscatter. We used a cube root transformation for the dependent variable (biomass) and combined SAR channels as the independent variable. The cube root transformation equalizes the variance and produces a normal distribution of biomass data (e.g., Ranson et al., 1997). The relationships between SAR backscatter values (in dB) and the cubic root of forest biomass were determined using linear regression. Measurements from 17 homogeneous stands large enough to provide representative radar signatures were used to develop the regression model. An additional 28 stands were used for testing. The equation using a combination of AIRSAR bands (i.e., PHV–CHV) was

$$b^{1/3}=2.186+0.259\ (\mathrm{PHV–CHV}), \qquad r^2=0.78. \qquad (1)$$

This relation [Eq. (1)] was used on a pixel by pixel basis to produce images of the predicted biomass from the AIRSAR images. To reduce the effects of speckle, the average backscatter value from an array of points were used as the center pixel backscatter value from which the biomass was calculated. The biomass map was also added to the GIS.

Forest Model Implementation

The forest model ZELIG (Urban, 1990), adapted as described in Levine et al. (1993), was used to simulate the successional dynamics of the southern boreal/northern hardwood forest transition zone found at the NEF. Because soil moisture is considered to be of primary importance in determining the structure (e.g., biomass and species composition) of these forests (Bonan and Shugart, 1989), waterlogging effects (adapted from Botkin, 1993) were included. This required connecting the ZELIG model to a soil physics model that simulates depth to saturated soils (see Weishampel et al., 1999). Diameter at breast height (dbh), height, height to base of crown, and foliage density were recorded for each individual tree in nine (10 m×10 m) ZELIG plots.

To implement the model, site parameters (e.g., soil fertility and monthly values of temperature and precipitation) and autecological parameters (e.g., height and diameter maxima and growth tolerances) were derived from empirical data and published sources (e.g., Pastor and Post, 1985; Botkin, 1993). Forest succession on 10 soil types (see Table 1) found at the NEF were simulated starting from bare soil. Depth to water table and available water holding content of the soil were derived using the FroST model (Levine and Knox, 1997). Parameters for 10 soil types mapped in the study area (Fig. 3) were used. The spatial scale of the ZELIG simulations were performed to represent a patch size of 30 m×30 m to correspond to the scale of typical remotely sensed data. This was done by running the model for nine spatially independent 10 m×10 m plots (Weishampel et al., 1999). Because gap models possess underlying stochasticity in their regeneration, mortality, and weather routines, 15 separate runs of the nine plots were performed to generate a range of stand responses from which stand averages were calculated. The simulation results were recorded at 5-year intervals up to 500 years.

Biomass for simulated trees was calculated from modeled dbh using allometric equations developed for central Maine, USA forests (Young et al., 1980). The average biomass was then determined for the simulated 30 m plots.

Predictive Images

The basis of modeling forest dynamics and tying the simulation to a real landscape is essentially a model initialization problem. Knowledge of the set of soil and vegetation attributes at the date of remote sensing imagery enables the prediction of future vegetation attributes for a given location based on the long-time series of ZELIG model results. Referring to Figure 2, attributes of soil type, forest biomass, and forest cover type are known, as described above. These known attributes are used to initialize the model for each location (pixel) in the remote sensing attribute and soil maps. Normally, model initialization requires explicit knowledge of the dbh distribution and species composition. This approach uses mapped attributes to identify the ZELIG simulation best representing the present state of a pixel location in terms of soil type, cover class, and biomass.

First the ZELIG model results were searched for soil type, vegetation classification type, and biomass level. To relate the SAR classification to the forest model results, only pixels classified as forest (i.e., hardwood, softwood, mixed, regeneration) and clearing were used. Pixels classified as regeneration were relabeled as hardwood since natural regrowth in disturbed areas is primarily deciduous species. In the case of the pixels identified as clearing, the original forest cover class is unknown so that the mapped soil type and matching biomass level are used to select the class. Areas mapped as bogs, wetlands, grass, and water were assumed not to change over the simulation period. Model results were coded as hardwood, softwood, and mixed forest based on the proportions of deciduous (e.g., aspen, birch, maple) and conifer (e.g., spruce, hemlock, pine, cedar) species. Mixed stands were labeled as those with less than 60% occurrence of hardwood or softwood. Biomass was calculated for a sim-

Table 1. Ten Soil Series and Associated Drainage and Taxonomic Classifications Found in the Maine Study Site and Used for Forest Model Simulations

Soil Series	*Drainage Class*	*Taxonomic Classification*
Adams	Somewhat excessively	Sandy, mixed, frigid Typic Haplorthod
Boothbay	Somewhat poorly	Fine-illitic, nonacid, frigid Andic Dystrochrept
Colonel	Somewhat poorly	Coarse-loamy, mixed, frigid Andic Dystrochrept
Croghan	Somewhat poorly	Sandy, mixed, frigid Aquic Haplorthod
Dixfield	Moderately well	Coarse-loamy, mixed, frigid Andic Dystrochrept
Kinsman	Very poorly	Sandy, mixed, frigid Aeric Haplaquod
Marlow	Well	Coarse-loamy, mixed, frigid Typic Haplorthod
Peacham	Very poorly	Coarse-loamy, mixed, frigid Typic Haplohumod
Scantic	Poorly	Fine-illitic, nonacid, frigid Typic Haplaquept
Westbury	Poorly	Coarse-loamy, mixed, frigid Aeric Haplaquod

ulated stand by using dbh based allometric equations that were developed for Maine forests species (Young et al., 1980).

The simulation with the matching soil type, matching class type, and minimum difference between mapped and modeled biomass was selected as the present state of a given pixel location. The simulation period was restricted to the first 200 years based on field observations of the forest age structure. The simulation period that most closely matched the known attributes became the initial stand age. Then the model results for the next 100 years were used for the prediction of forest attributes of biomass and forest type at that pixel location.

Under certain conditions, no ZELIG simulation run matched the mapped set of attributes for a pixel location. If no simulation runs were found that matched both the soil type and cover type, then the pixel was labeled as "nomatch" and is not included in further analyses. In addition, if the forest class was matched, but the biomass difference was larger than 5 kg/m^2, then this pixel is labeled as "unknown" and not included for further analyses. The possible reasons for no-match and unknown conditions include: The soil map is wrong for a particular location; the ZELIG model does not grow trees of a certain species on a particular soil, although the species is actually found there; and remote sensing forest classification and biomass values for the pixel are incorrect. The "unknown" and "no-match" classes comprise about 9% of the image.

RESULTS

Remote Sensing Analysis

Maps of forest type and biomass were developed from the AIRSAR data (not shown). The forest type classification results from the AIRSAR data compare favorably with the with field information (Ranson and Sun, 1997). Briefly, all non-forest classes were 100% correctly identified. Forest type classification for softwood was 94% correct. Hardwood showed 86.5% correct classification and mixed forest showed 84.0% correct classifications.

Biomass estimation results were also consistent with ground observations. Comparing biomass predicted with Eq. 1 against the 28 field measurements resulted in Eq. (2):

$$\text{Predicted}_{\text{biomass}} = 1.954 + \text{Measured}_{\text{biomass}} * 1.064, \qquad r^2 = 0.87. \tag{2}$$

We found that the biomass method worked best for biomass values below 15 kg/m^2.

Forest Modeling

Figure 4 presents the average biomass trajectories simulated from 15 30 m× 30 m (900 m^2) stands growing on three of the 10 NEF soil types used in the simulation. The range of biomass simulations illustrates the importance of considering soil types in our study area. Generally, well or moderately well-drained soils (e.g., Dixfield in Fig. 4) produced higher biomass values in less time, whereas poorly drained soils required much more time to establish maximum biomass values. Soil type also controlled the forest type composition with better drained soils establishing significant proportions of hardwoods (e.g., Dixfield, Fig. 4). Poorly drained soils tended to have populations dominated by softwoods (e.g., Kinsman, Fig. 4), although somewhat poorly well drained soils such as Colonel (Fig. 4) were populated by hardwoods at early successional stages. Because of the stochastic timing of tree birth and death, replicate simulations can exhibit considerable variation about the averages shown in Figure 4. The simulated biomass trends and the underlying patterns of dominance by softwood and hardwood species were consistent with field measurements reported by Ranson and Sun (1994a,b) and Levine et al. (1994). A total of 15,000 simulations were recorded (10 soil types×15 replications×100 time steps).

Using the forest type, biomass, and soil maps to initialize the forest succession model produced the forest

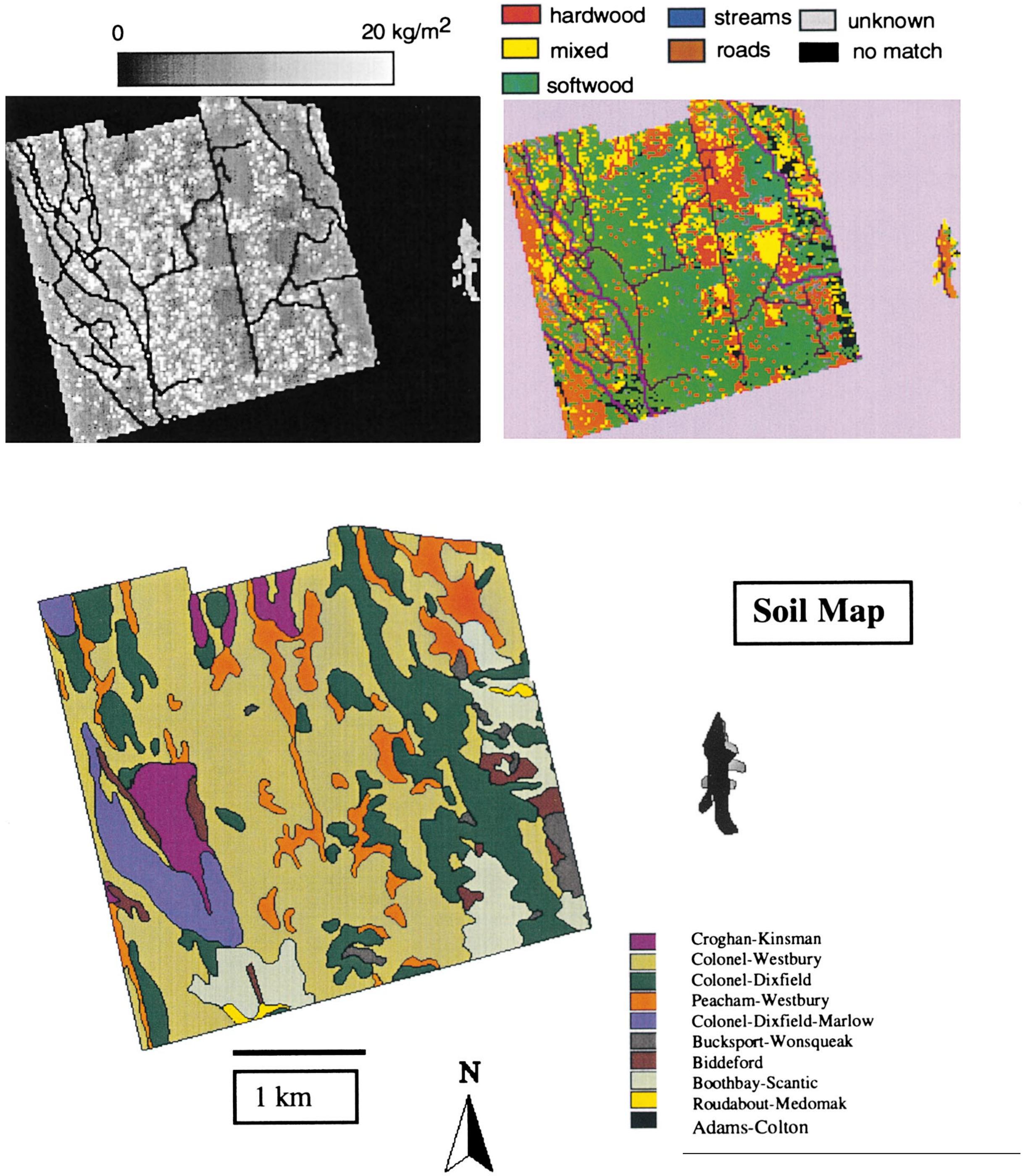

Figure 3. Maps of forest type (top right), above-ground biomass (top left) developed from remote sensing analysis and the ZELIG model (bottom) soil survey map. These maps define the initial conditions for spatially explicit forest growth model simulations.

type and biomass images shown in Figure 3. These maps cover an area where detailed soils information was available within in the study area, including the small isolated area to the east (see soil map in Fig. 3). This area was included in the mapping because it is located on an esker with somewhat excessively well-drained soils not found elsewhere in the study area. The initialization results were consistent with the remote sensing images except in the cases of no-match and unknown pixels as seen in Figure 3. This indicates that this approach can be used to simulate the initial condition of the landscape in our study area.

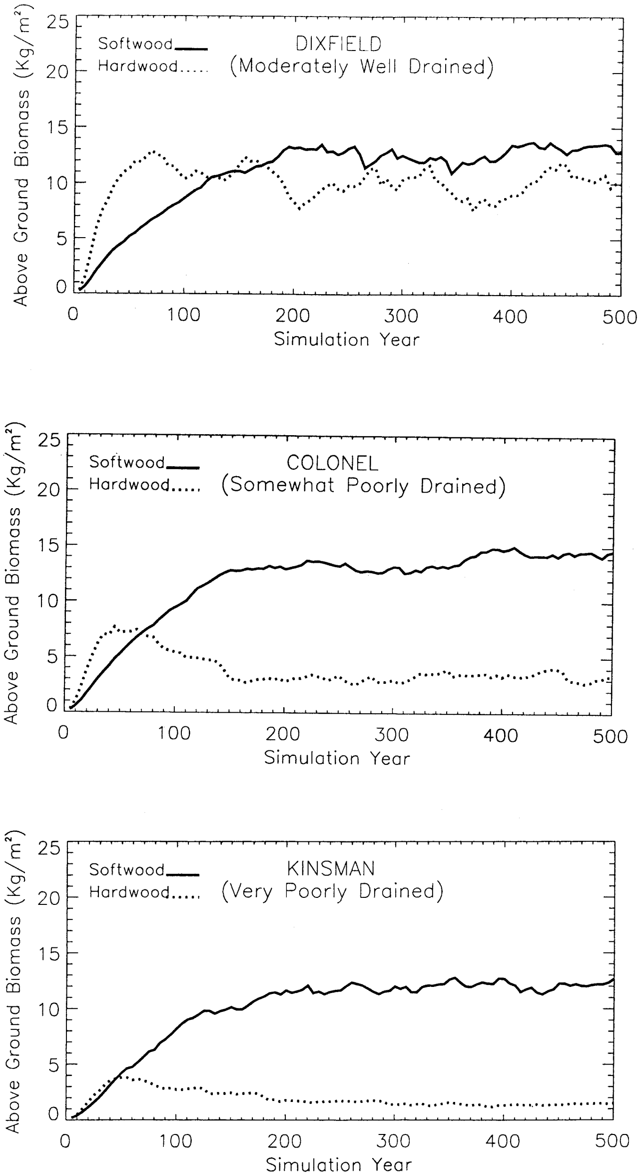

Figure 4. Example results of the forest simulation model (ZELIG) with mean yearly biomass of softwood and hardwood forest stands growing on soils with different drainage classes. The biomass trajectories illustrate the effect of soil type on the analysis.

As discussed above, about 9% of the pixels covering the study area fell outside the simulation results and were classified as unknown or no-match (see Fig. 3). The majority of no-match pixels were classified as hardwood on soils that, according to the forest succession model results, cannot sustain hardwood forest. For example, 224 pixels were classified as low biomass (<10 kg/m^2) hardwood growing on very poorly drained Kinsman soil. From Figure 4 (Dixfield soil) it can be seen that this condition should not occur because of the need for a better drained soil to support hardwood stands. In one instance, the SAR classification labeled a stand as hardwood growing on a poorly drained soil again resulting in a no-match condition. Inspection of available forest cover maps revealed this stand to consist of northern white cedar, a conifer or softwood species. This forest type was not trained for in the classification procedure. In this case the forest modeling helped improve the forest classification. For unknown pixels, most were classified as low biomass softwoods growing on soils where the forest model shows the class should be hardwood. For example, one can see from Figure 4 that forests on the Dixfield soil type will most likely be dominated by hardwoods over the first 50 years of growth.

Predictive Images

The predictive images can be used to assess forest dynamics as the change in forest type and biomass over time. Assuming that no areas of forest are harvested during the 100-year period (although this can be included in the analysis), the forest can be expected to develop, under current climate conditions, as shown in Figure 5 and Table 2. Average biomass, accumulated over forest type, increased by about 50% over the first 25 years and then increased slowly over the next 50-year period with a gradual decrease in standard deviation. These results indicate that the forest is mostly mature, slowly growing stands. Hardwood biomass increased the most over the 100-year period but, because of the very small area covered, contributed minimally to the total biomass.

The trends in forest types seen in Figure 5 and Table 2 indicate that the hardwood stands change into mixtures of hardwood and softwood or into softwood stands. The percentage of mixed stands increases during the first 50 years and then declines over the next 50 years. This is consistent with observations of the forest in central Maine. The forest types of recently disturbed areas generally start out as hardwood or mixtures then develop into softwoods. Poorly drained soils support stands of softwood, while well-drained soils sustain development of hardwoods. Existing stands of hardwoods on the site are growing on fire disturbed areas and are mostly nearing maturity and subsequent decadence. Of course, detailed analyses of individual stands are required to confirm that these observations are valid at the local level

Since the initialization procedure assumes that the age of the stand on a given soil type can be estimated from the forest type and biomass level for a known soil, it is instructive to examine areas of known age in the study area. Age data is difficult to compile, but we had two sources of information available. Timber harvesting in the form of clear cutting has been conducted in the imaged area since 1982. Comparing the initialization age with the age of these clearings reveals if the technique can be used to estimate the age of young stands. The

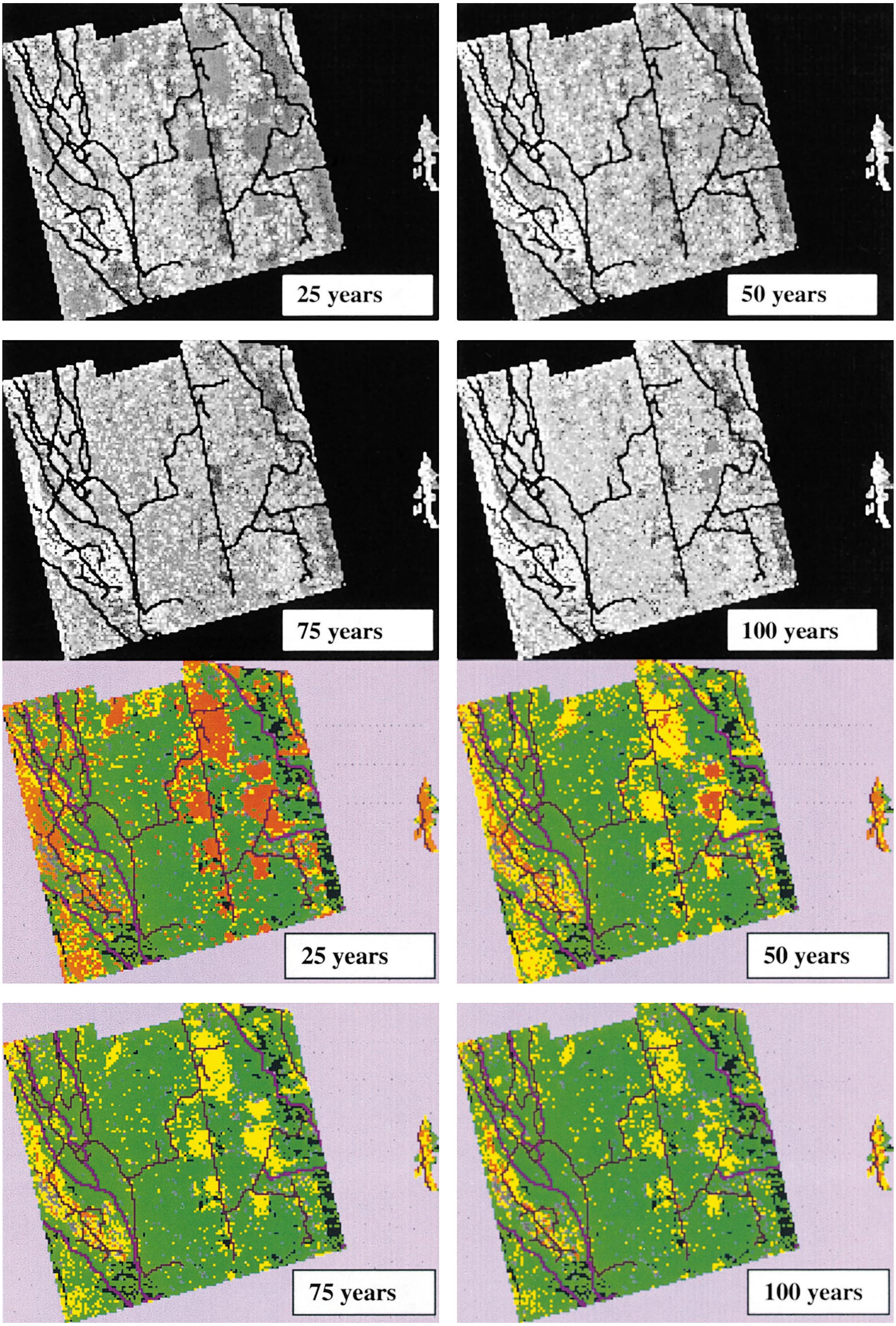

Figure 5. Predictive maps developed from remote sensing and ecosystem modeling for 25, 50, 75 and 100 years from remote sensing data acquisition (1994). (Upper) forest type; (Lower) biomass map. See Figure 3 for map legends. North is at top. Image area is about 6 km×6 km.

Table 2. Simulated Forest Type and Average Biomass for Forest Areas in Study Area over a 100-Year Simulation Period

Forest Type	Simulation Year 0	25	50	75	100
	Percent of Forested Area				
Hardwood	23.4	22.0	5.7	1.1	0.9
Softwood	61.5	65.7	70.6	79.0	85.1
Mixed	15.2	12.2	23.7	20.0	14.0
	Forest Type Biomass—Mean, kg/m^2 (Std. Dev., kg/m^2)				
Hardwood	5.3 (4.1)	11.5 (2.0)	17.3 (2.5)	20.8 (2.6)	23.4 (4.6)
Softwood	10.6 (4.5)	12.0 (3.9)	14.2 (3.1)	14.8 (2.8)	16.0 (3.5)
Mixed	4.5 (4.9)	14.5 (4.9)	14.0 (2.6)	16.4 (3.1)	17.1 (3.1)
Combined	8.5 (4.5)	12.2 (3.7)	14.3 (2.9)	15.1 (2.8)	16.3 (3.4)

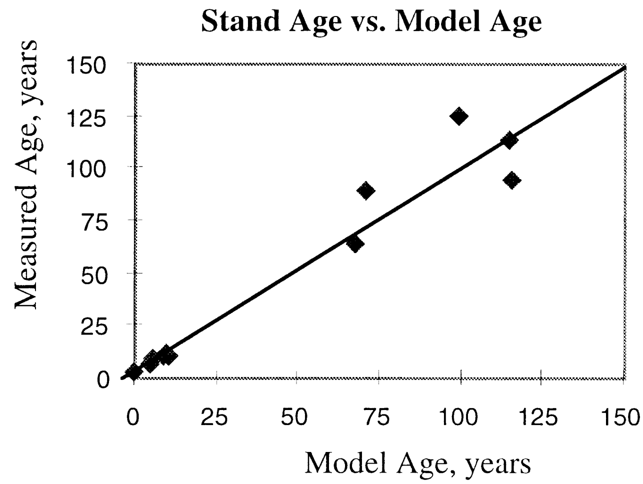

Figure 6. Comparison of measured stand mean age with model results.

second source of age data was measurement from five plots acquired by GSFC personnel in the spring of 1994. For these data the same measurements were acquired as for the biomass estimation method described above. In addition, two codominant trees in each of nine sample plots were cored, and the tree rings analyzed later in a laboratory. Up to 18 samples were available for each plot in each site. These sites were located on a map of stand age produced from the model initialization. That is, each pixel value represents the age of the stand selected from the model simulations based on forest type, biomass, and soil type. A 3×3 array of pixels were extracted from the image and averaged to estimate the predicted age for a site. Figure 6 presents a plot of the measured and modeled height results. The data values are clustered at the young ages for the clear cut data and at older ages from the sample plot data; therefore, no attempt was made to develop a statistical relationship. However, the scatter of the data about the 1 to 1 line is small. These results are promising and indicate this technique may be suitable for estimating stand age for the purpose of model initialization.

SUMMARY

A procedure to use forest type and biomass maps developed from remote sensing data to initialize a forest growth model for a northern forest in Maine, USA was described. The remotely sensed forest attributes were used together with a soils map to identify the stand age within a forest model simulation. This approach enabled the development of predictive maps of forest type and biomass for up to 100 years in the future. Longer periods can be examined by extending the duration of the model runs.

AIRSAR data was used in this study because of its availability during the times of our ground measurements, and reasonable forest attribute maps could be developed. It should be emphasized that these data were used as proof of concept and that the extension of the results to other forests should not require AIRSAR data. Landsat data should be suitable for forest cover type applications as demonstrated by He and Mladenoff (1999). Hall et al. (1997) describe a technique to estimate coniferous forest biomass with Landsat data. Other successful above-ground biomass mapping has been demonstrated mostly with multipolarization and multifrequency SARs (e.g., Le Toan et al., 1992; Dobson et al, 1992; Ranson and Sun, 1997). The P-band radar available on AIRSAR can be used to improve biomass estimates of forests, but unfortunately it will not be available for broad scale coverage in the foreseeable future. There are plans to launch multipolarization C-band radars (ASAR: Europe and Radarsat-2: Canada) and a multipolarization L-band radar (ALOS: Japan) within the next few years. In addition, new Lidar technology such as NASA's Vegetation Canopy Lidar promises to improve biomass estimates in the near future.

The results presented are reasonable in terms of the initial forest classification and biomass estimates. A preliminary analysis of stand age and predicted age also indicates that the technique presented here is valid. Despite the uncertainties of the actual soil type for a pixel and errors in the remote sensing maps the results demonstrate the potential for using remote sensing in combination with ecosystem models to simulate forest dynamics. The technique could be used to augment ground data in remote area if the model can be parametrized for the appropriate soil and forest type. The forest growth model can also indicate the likely type of forest growing on a particular soil. This information can be used to improve the classification of remotely sensed data. Additional stand age related variables such as leaf area index and canopy height can be added to the procedure by inclusion of appropriate remote sensing data sets such as Landsat and eventually the Vegetation Canopy Lidar.

This approach is also amenable to studying carbon flux dynamics as they are controlled by forest structure. More realistic dynamics may be provided by models that explicitly follow the carbon budgets of individual trees (e.g., Friend et al., 1997). Since forest type maps and biomass maps can be generated for any set of simulation conditions, the approach described may be useful for understanding the effects of management practices on forests and the response of forest dynamics to changing climate. The technique of using coupled models and remote sensing will be applied to data sets that cover larger areas of boreal forests in the USA and Canada.

This work was supported in part by NASA's Earth Science Enterprise through the Terrestrial Ecology Program and the former SIR-C/XSAR Project.

REFERENCES

Bidlake, W. R., Campbell, G. S., Papendick, R. I., and Cullum, R. F. (1992), Seed-zone temperature and moisture conditions under conventional and no-tillage in Alaska. *Soil Sci. Soc. Am. J.* 56:1904–1910.

Bolin, B. (1986), How much CO_2 will remain in the atmosphere. In *The Greenhouse Effect, Climate Change and Ecosystems (SCOPE 29)* (B. Bolin, B. R. Doos, J. Jager, and R. A. Warrick, Eds.), Wiley, Chichester, 541 pp.

Bonan, G. B., and Shugart, H. H. (1989), Environmental factors and ecological processes in boreal forests. *Annu. Rev. Ecol. Systematics* 20:1–28.

Bonan, G. B., Chapin, F. S., and Thompson, S. L. (1995), Boreal forest and tundra ecosystem as components of the climate system. *Clim. Change* 29:145–167.

Botkin, D. B. (1993), *Forest Dynamics: An Ecological Model*, Oxford University Press, New York.

Deutschman, D. H., Levin, S. A., Devine, C., and Buttel, L. A. (1997), Scaling from Trees to Forests: Analysis of a Complex Simulation Model, Science 277:1688.

Dobson, M. C., Ulaby, F. T., Le Toan, T., Beaudoin, A., Kasischke, E. S., and Christensen, N. (1992), Dependence of radar backscatter on coniferous forest biomass. *IEEE Trans. Geosci. Remote Sens.* 30:412–415.

Friend, A. D., Stevens, A. K., Knox, R. G., and Cannell, M. G. R. (1997), A process-based, terrestrial biosphere model of ecosystem dynamics (Hybrid 3.0). *Ecol. Model.* 95: 249–287.

Goward, S. N., Williams, D. L., and Peterson, D. L. (1994), NASA multisensor aircraft campaigns for the study of forest ecosystems. *Remote Sens. Environ.* 47:107–108.

Hall, F. G., Knapp, D. E., and Huemmrich, K. F. (1997), Physically based classification and satellite mapping of biophysical characerisitics in the southern boreal forest. *J. Geophys. Res.* 102(D24):29,567–29,580.

He, S. H., and Mladenoff, D. L. (1999), Spatially explicit and stochastic simulation of forest-landscape fire disturbance and succession. *Ecology* 80(1):81–99.

Kasischke, E. S., and Christensen, N. L. (1990), Connecting forest ecosystem and microwave backscatter models. *Int. J. Remote Sens.* 11:1277–1298.

Kimes, D. S., Ranson, K. J., and Sun, G. (1977), Inversion of a forest backscatter model using neural networks. *Int. J. Remote Sens.* 18:2181–2199

Knox, R. G., Kalb, V., and Levine, E. R. (1997), A problem solving workbench for interactive simulation of ecosystems. *IEEE Comput. Sci. Eng.* 4(3):52–60.

Levine, E. R., and Knox, R. G. (1997), Modeling soil temperature and snow dynamics in northern forests. *J. Geophys. Res.* 109:29,407–416.

Levine, E. R., Ranson, K. J., Smith, J. A., et al. (1993), Forest ecosystem dynamics: linking forest succession, soil process and radiation models. *Ecol. Model.* 65:199–219.

Levine, E. R., Knox, R. G., and Lawrence, W. (1994), Relationships between soil properties and vegetation at the Northern Experimental Forest, Howland, Maine. *Remote Sens. Environ.* 47:231–241.

Le Toan, T., Beaudoin, A., Riom, J., and Guyon, D. (1992), Relating forest biomass to SAR data, *IEEE Trans. Geosci. Remote Sens*. 30:403–411.

Moik, J. G. (1980), *Digital Processing of Remotely Sensed Images*, NASA SP-431, Science and Technical Information Branch, NASA, Greenbelt, MD, 327 pp.

Myneni, R. B., Keeling, C. D., Tucker, C. J., Asrar, G., and Nemani, R. R. (1997), Increased plant growth in the northern latitudes from 1981–1991. *Nature* 386:698–702

Pastor, J., and Post, W. M. (1985), *Development of a Linked Forest Productivity-Soil Process Model*, ORNL/TM-9519, Oak Ridge National Laboratory, Oak Ridge, TN.

Pastor, J., and Post, W. M. (1988), Response of northern forests to CO_2 induced climate change. *Nature* 334:55–58.

Pastor, J., and Mladenoff, D. J. (1992), The southern boreal-northern harwood forest border. In *Systems Analysis of the Global Boreal Forest* (H. H. Shugart, R. Leemans, and G. B. Bonan, Eds.), Cambridge University Press, New York, pp. 216–240.

Ranson, K. J., and Sun, G. (1994a), Northern forest classification using temporal multifrequency and multipolarimetric SAR images. *Remote Sens. Environ.* 47:142–153.

Ranson, K. J., and Sun, G. (1994b), Mapping biomass for a northern forest using multifrequency SAR data. *IEEE Trans. Geosci. Remote Sens.* 32:388–396.

Ranson, K. J., and Sun. G. (1997), An evaluation of AIRSAR and SIR-C/X-SAR data for estimating northern forest attributes. *Remote Sens. Environ.* 59:203–222.

Ranson, K. J., Smith, J. A., Sun, G., Weishampel, J. F., and Knox, R. G. (1997), Forest biomass from combined ecosystem and radar backscatter modeling. *Remote Sens. Environ.* 59:118–133.

Rignot, E., Way, J., Williams, C., and Viereck, L. (1994), Radar estimates of above ground biomass in boreal forests of interior Alaska. *IEEE Trans. Geosci. Remote Sens*. 32:1117–1124.

Shugart, H. H., Smith, T. M., and Post, W. M. (1992), The potential for application of individual-based simulation models for assessing the effects of global change. *Annu. Rev. Ecol. Systematics* 23:15–38.

Trumbore, S. E.; Chadwick, O. A., and Amundson, R. (1996), Rapid exchange between soil carbon and atmospheric carbon dioxide driven by temperature change. *Science* 272: 393–396.

Urban, D. L. (1990), *A Versatile Model To Simulate Forest Pattern: A Users Guide to ZELIG, Version 1.0*, Environmental Sciences Department, University of Virginia, Charlottesville, VA.

Way, J. B., and Smith, E. A. (1991), The evolution of synthetic aperture radar systems and their progression to the EOS SAR. *IEEE Trans. Geosci. Remote Sens.* 29:962–985.

Weishampel, J. F., Knox, R. G., and Levin, E. R. (1999), Soil saturation effects on forest dynamics: scaling across a southern boreal/northern hardwood landscape. Landscape Ecology 14:121–135

Young, H. E., Ribe, J. H., and Wainwright, K. (1980), Weight tables for tree and shrub species in Maine, Misc. Report 230, Life Sciences and Agriculture Experiment Station, University of Maine, Orono, September.